Journal of Molecular Liquids 178 (2013) 160–167

Contents lists available at SciVerse ScienceDirect

Journal of Molecular Liquids

journal homepage: www.elsevier.com/locate/molliq

Twisted intramolecular charge transfer effects on fast violet B and fast blue RR: Effect of HP-α- and HP-β-cyclodextrins

M. Jude Jenita, G. Venkatesh, V.K. Subramanian, N. Rajendiran *

Department of Chemistry, Annamalai University, Annamalai Nagar-608 002, Tamilnadu, India

ARTICLE INFO

Article history:
Received 3 April 2012
Received in revised form 27 November 2012
Accepted 28 November 2012
Available online 11 December 2012

Keywords:
Fast violet B
Fast blue RR
Cyclodextrin
TICT
Inclusion complex
PM3 method

ABSTRACT

Absorption, steady state and time resolved fluorescence spectra of fast blue RR (FBRR) and fast violet B (FVB) were studied in hydroxypropyl-α-cyclodextrin (HP-α-CD) and hydroxypropyl-β-cyclodextrin (HP-β-CD). Dual emission observed in both CDs suggested that twisted intramolecular charge transfer (TICT) is present in both molecules. The normal Stokes shifted bands originated from the locally excited state and the large Stokes shifted bands were due to the emission from a TICT state. The ratio of the TICT to the normal emission increased with HP-β-CD concentration, while it was constant upon addition of HP-α-CD. This behavior was in accordance with CD dependent decay times of the TICT and normal emissions, indicating the formation of different 1:1 FVB/CD and FBRR/CD inclusion complexes. The benzoyl moiety of FVB/FBRR was deeply encapsulated in the HP-β-CD cavity, whereas in HP-α-CD, it was exposed to the water phase. Semiempirical quantum optimization was also carried out to assign the encapsulation of the FBRR and FVB.

1. Introduction

Cyclodextrins (CDs) are macrocyclic alpha-1,4-maltooligosaccharides consisting of D-(+)-glucopyranose units. With their special molecular structures, they are capable of incorporating various organic compounds into their nanocavities and affecting the physical and chemical properties of incorporated compounds. Thus, CDs have been used in many fields such as foods, cosmetics, toiletries, agrochemicals and inclusion of pharmaceuticals guest molecules [1,2]. Among CDs, α-CD, β-CD and γ-CD that composed of six, seven and eight glucopyranose units respectively are the most popular. Many researchers have studied the interaction of β-CD with drugs and the corresponding thermodynamic parameters by conductance [3–5], surface tension [4–7], spectroscopy [8–13] and other methods [14,15]. However, only very few reports dealt with structural analysis of supramolecular inclusion complexes of hydroxypropyl-α-cyclodextrin (HP-α-CD) and hydroxypropyl-β-cyclodextrin (HP-β-CD) with drug molecules [16,17].

Recently, we studied many molecules in which the proton donor groups were $-NH_2$ and $-OH$ but the proton acceptor groups were N═N, ═N−, C═O, etc. In our earlier studies, fast violet B [18], 2-amino-3-benzyloxypyridine [19], azo [20], sulphanilamides [21], hydroxy benzaldehyde [22] and amino benzoic acid [23] molecules were investigated. In the present work, the electron acceptor group is the benzoyl moiety and donor group is the amino and methoxy groups. Because the CO group is a better electron acceptor than $-SO_2-NH-$, it might facilitate the formation of the twisted intramolecular charge transfer (TICT) in fast violet B (FVB, 4-amino-5-methoxy-2-methylbenzanilide) and fast blue RR (FBRR, 4-amino-2,5-dimethoxybenzanilide or 4-benzoylamino-2,5-dimethoxyaniline) than sulphanilamides and hydroxybenzaldehyde. The main aims of the present study were: (i) to compare the effects of the electron-withdrawing in FVB and FBRR molecules on the TICT emission, and (ii) to study if the inclusion complexes increase or decrease the longer wavelength (LW) emission. The results were analyzed by the UV–visible, steady state and time resolved fluorescence, FTIR, ^{1}H NMR and molecular modeling.

2. Materials and methods

2.1. Reagents and materials

FBRR, FVB, HP-α-CD and HP-β-CD were purchased from Aldrich Chemical and used without further purification. Triply distilled water was used for the preparation of aqueous solutions. Aqueous solutions with pH below 2.0 and above 11.5 were prepared by adding appropriate amounts of dilute (~10^{-3} M) solutions of NaOH and H_3PO_4. All spectral measurements were performed at a solute concentration of 2×10^{-5} M. The concentrations of HP-α-CD and HP-β-CD solutions varied from 1×10^{-3} to 1×10^{-2} M.

2.2. Instruments

Absorption spectral measurements were performed with a Shimadzu UV 1601 PC model UV–visible spectrophotometer and steady-state fluorescence measurements were made using a Shimadzu model RF-5301 spectrofluorimeter. The pH of the solutions was measured using Elico

---

* Corresponding author. Tel.: +91 94866 28800 (mobile); fax: +91 4144 238080.
E-mail address: drrajendiran@rediffmail.com (N. Rajendiran).

0167-7322/$ – see front matter © 2012 Elsevier B.V. All rights reserved.
http://dx.doi.org/10.1016/j.molliq.2012.11.033

model LI-120 pH meter. FT-IR spectral measurements were obtained with Avatar-330 FT-IR spectrometer using KBr pelleting. The range of spectra was from 400 to 4000 cm^{-1}. A Bruker Advance DRX 400 MHz superconducting NMR spectrophotometer was used to obtain ^1H NMR spectra. The fluorescence lifetime measurements were performed using a Jobin-Yvon IBH picosecond laser instrument. A diode pumped Millenia CW laser (Spectra Analysis) 532 nm was used to pump the Ti–Sapphire rod in a Tsunami picosecond mode locked laser system (Spectra physics model 4690 M3S). The Ti–Sapphire rod was oriented at Brewster's angle to the laser beam. The wavelength turning range was 280–540 nm (i.e, standard pico configuration). The fluorescence decay of the sample was analyzed using IBH data analysis software. The fluorescence decay profiles were fitted to the expressions:

$$I(t) = A_1 \exp\left(\frac{-t}{\tau^1}\right) + A_2 \exp\left(\frac{-t}{\tau^2}\right) \tag{1}$$

$$I(t) = A_1 \exp\left(\frac{-t}{\tau^1}\right) + A_2 \exp\left(\frac{-t}{\tau^2}\right) + A_3 \exp\left(\frac{-t}{\tau^3}\right) \tag{2}$$

where τ_1, τ_2 and τ_3 are the lifetimes of the three components; A_1, A_2 and A_3 are the corresponding pre-exponential factors and t is time. The average fluorescence lifetime was calculated using the equation

$$\langle \tau \rangle = \sum \tau_i A_i \tag{3}$$

2.3. Molecular modeling studies

The theoretical calculations were performed using Gaussian 03W. The calculations were carried out in the gas phase, so solvent effects were not taken in the calculations. The initial geometries of the guest and CD molecules were constructed with Spartan 08 and then optimized by PM3 method. HP-α-CD and HP-β-CD were fully optimized by PM3 without any symmetry constraints [24–26]. Because the semi-empirical PM3 method has been shown to be a powerful tool in the conformational study of cyclodextrin complexes and has high computational efficiency in calculating CD systems [24–26], it was selected to study the inclusion process of HP-α-CD and HP-β-CD with FBRR and FVB in this work.

3. Results and discussion

3.1. Absorption studies

Fig. 1 shows the absorption spectra FBRR in aqueous solutions with different concentrations of HP-α-CD and HP-β-CD. It was evident that the absorbance of FVB and FBRR increased with the increasing concentration of both CD molecules. It has been well established that the enhanced/decreased absorbance of guests in the presence of CD molecules is due to the formation of inclusion complexes [27–32]. Guest molecules can be included into the CD cavity depending upon their size, geometry and hydrophobicity. Of the two CDs used in this study, HP-α-CD has smaller cavity size (~5.6 Å) than HP-β-CD (~6.5 Å), however, both the CDs have similar height (~7.8 Å). FVB and FBRR molecules have an average length of ~12.2 Å and width of ~7.5 Å (methoxy and methyl group bond distances). The small variation in the absorbance of FVB and FBRR in HP-α-CD is probably due to smaller cavity size and therefore, lack of complexation. On the other hand, the cavity size of HP-β-CD is sufficiently wider to form a stable inclusion complex with the guest compounds. The deep inclusion of the FVB/FBRR in HP-β-CD than that of HP-α-CD may be due to the strong hydrogen bonding ability of the alcoholic OH on the CD ring with the –CONH– group of the guests.

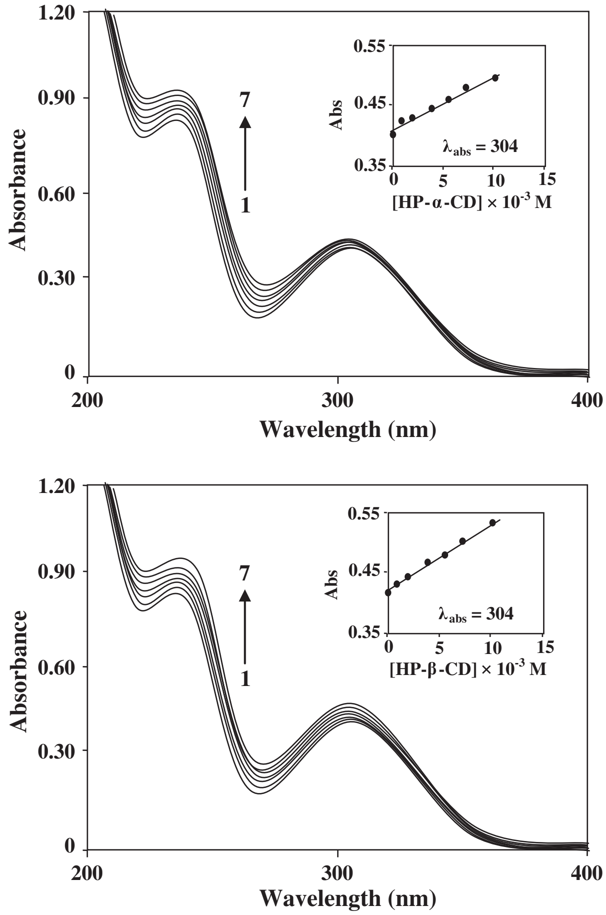

Fig. 1. Absorption spectra of FBRR in different HP-α- and HP-β-CD concentrations (M): 1) 0, 2) 0.001, 3) 0.002, 4) 0.004, 5) 0.006, 6) 0.008 and 7) 0.01. Inset figure: absorbance vs HP-α- and HP-β-CD concentrations.

Among the two CDs, HP-β-CD has the highest solubility as well as largest binding constant with the guests; the difference in the binding constant is due to the difference in absorbance that may be attributed to the difference in their inclusion. The most likely orientation of guest which can explain the hydrophobicity is one in which the benzoyl ring is non-coplanar with the aniline ring through strong intermolecular hydrogen bonding. The absorbance bands were broad, which suggested that the aniline ring is not in the plane of the benzoyl ring and the dipole for the FVB/FBRR is higher in the inclusion complexes.

The binding constant of the FVB/FBRR obtained by the absorbance data suggested that the binding of FVB/FBRR is weak in HP-α-CD than that of HP-β-CD. The binding constants obtained by absorbance were lower than those obtained from fluorescence studies. Since both methods measure ground and excited state phenomenon respectively, the values obtained by the above techniques may reflect structural differences in the guest molecule. The low binding constant of FVB/FBRR with HP-α-CD indicated that the polar substituent of the molecule and the higher binding constant in HP-β-CD implied that this cavity is less polar than that of HP-α-CD.

3.2. Fluorescence studies

Fig. 2 shows the fluorescence spectra of FBRR in aqueous solution as a function of HP-α-CD or HP-β-CD concentration, excited at 310 nm, where the CD dependent absorbance change is negligible. In the absence of CD solution, the dual fluorescence of TICT was observed even though the emission quantum yields of the normal emission around 350 nm and the TICT around 455 nm were very low. The